Vapour - Liquid Equilibrium and Thermodynamic Properties of Refrigerants R143a and R152a from Cubic Equations of State

VIOREL FEROIU*, DAN GEANA*

Politehnica University Bucharest, Department of Applied Physical Chemistry and Electrochemistry, 1 Polizu Str., 011061 Bucharest, Romania

Vapour - liquid equilibrium and thermodynamic properties were predicted, along the saturation curve and in the single-phase region for refrigerants R143a (CF_3CH_3) and R152a (CHF_2CH_3). Five cubic equations of state were used: Soave-Redlich-Kwong (SRK), Peng-Robinson (PR), Schmidt-Wenzel (SW), Freze et al. (C1) and GEOS3C. A wide comparison with experimental data was made. So far GEOS3C, with three estimated parameters, compares favorably to other equations in literature, being simple enough for applications.

Keywords: *equation of state, vapour - liquid equilibrium, thermodynamic properties, refrigerants.*

Refrigerants are the working fluids in refrigeration, air-conditioning and heat pumping systems. They absorb heat from one area, such as an air-conditioned space, and reject it into another, such as outdoors, usually through evaporation and condensation, respectively. A refrigerant must satisfy many requirements: chemical stability, transfer heat ability, low toxicity, efficiency, reduced environmental consequences. Chemical stability under conditions of use is the most important characteristic. Safety codes may require a nonflammable refrigerant of low toxicity for some applications. The environmental consequences of a refrigerant that leaks from a system must also be considered. Because of their great stability, fully halogenated compounds, such as chlorofluorocarbons (CFCs), persist in the atmosphere for many years and eventually diffuse into the stratosphere. The molecules of CFCs, contain only carbon and the halogens chlorine and fluorine. Once in the upper atmosphere, CFC molecules break down and release chlorine, which destroys ozone (ozone depletion). In the lower atmosphere, these molecules absorb infrared radiation, which may contribute to the warming of the earth. Substitution of a hydrogen atom for one or more of the halogens in a CFC molecule greatly reduces its atmospheric lifetime and lessens its environmental impact. These compounds are called hydrochlorofluorocarbons (HCFCs).

In the last years, the hydrofluorocarbons (HFCs) are used as refrigerants, owing to their low ozone depletion potential.

No single fluid satisfies all the attributes desired of a refrigerant; as a result, a variety of refrigerants is used. Refrigerant selection involves compromises between conflicting desirable thermodynamic properties. In the classical thermodynamic framework it is possible to develop relations to calculate the Helmholz and Gibbs energies, enthalpies, entropies, fugacity coefficients and other thermodynamic properties of fluids. Such relationships together with equations of states (EOS) can be applied to obtain estimation techniques for thermodynamic property departure functions [1]. Then the "true" thermodynamic properties are calculated for pure components and mixtures.

The development of models for representation and prediction of physical properties and phase equilibria as well as the improvement of current equations of state (EOS) is of particular interest for the refrigeration industry [2-5]. In our previous works [6-8], thermodynamic properties of pure refrigerants and refrigerant mixtures were predicted by cubic equations of state.

In this work, vapour - liquid equilibrium and thermodynamic properties were predicted, along the saturation curve and in the single-phase region for two hydrofluorocarbons: **R143a** (CF_3CH_3) and **R152a** (CHF_2CH_3). Five cubic equations of state were used: Soave-Redlich-Kwong (SRK) [9], Peng-Robinson (PR) [10], Schmidt-Wenzel (SW) [11], Freze et al. (C1) [12] and GEOS3C [13]. A wide comparison with recommended NIST (National Institute of Standard and Technology, USA) data [14], considered as experimental data, was made. So far GEOS3C, with three estimated parameters, compares favorably to other equations in literature, being simple enough for applications.

The GEOS3C equation of state

The GEOS3C equation of state is a general form [1, 6] for the cubic equations of state with two, three and four parameters:

$$P = \frac{RT}{V-b} - \frac{a(T)}{(V-d)^2+c} \tag{1}$$

The four parameters a, b, c, d for a pure component are expressed by:

$$a = a_c\,\beta^2(T_r); \quad a_c = \Omega_a \frac{R^2T_c^2}{P_c}; \quad b = \Omega_b \frac{RT_c}{P_c};$$
$$c = \Omega_c \frac{R^2T_c^2}{P_c^2}; \quad d = \Omega_d \frac{RT_c}{P_c}; \tag{2}$$

The GEOS3C equation is based on the GEOS equation [15] and uses a new temperature function:

$$\beta(T_r) = 1 + C_1\,y + C_2\,y^2 + C_3\,y^3 \qquad \text{for } T_r \le 1 \tag{3}$$

$$\beta(T_r) = 1 + C_1\,y \qquad \text{for } T_r > 1 \tag{4}$$

$$y = 1 - \sqrt{T_r} \tag{5}$$

---

* *email: v_feroiu@chim.upb.ro; d_geana@chim.upb.ro*

The expressions of the parameters Ω_a, Ω_b, Ω_c, Ω_d are:

$$\Omega_a = (1-B)^3; \quad \Omega_b = Z_c - B; \quad \Omega_c = (1-B)^2(B-0.25); \quad \Omega_d = Z_c - 0.5(1-B) \tag{6}$$

$$B = \frac{1+C_1}{\alpha_c + C_1} \qquad \alpha_c \text{ - Riedel's criterion} \tag{7}$$

Using experimental values of the critical constants and the acentric factor for the calculation of α_c from the equation:

$$\alpha_c = 5.808 + 4.93\text{w} \tag{8}$$

the C_1, C_2 and C_3 parameters were estimated by constraining the equation of state to reproduce the experimental vapor pressure and liquid volume on the saturation curve.

The following features of GEOS3C parametrisation are important:

- it gives exactly the experimental critical point of any substance, and also the experimental critical compressibility factor Z_c;
- the prediction of liquid volume is improved, without translation, by the parameter C_1 from the temperature function of the attractive term;
- the three parameters C_1, C_2 and C_3 can provide very well the saturation pressure curve;
- the involving of the parameter C_1 in the expressions of a and b, leads to a "coupling" between the repulsive and attractive terms in a cubic equation of state.

As pointed out previously [6], the relations (6) are general forms for all the cubic equations of state with two, three and four parameters. Our software used in calculations is based on these equations for the reduction of GEOS to different cubic EOS from the literature. This is the meaning of the statement "general cubic equation of state" used for GEOS.

The following equations of the departure (residual) functions from ideal gas state at the same temperature and pressure were used with the GEOS equation (or GEOS3C) [16]:

$$\Delta U^R = -\left(a - T\frac{\partial a}{\partial T}\right)E \tag{9}$$

$$\Delta H^R = -\left(a - T\frac{\partial a}{\partial T}\right)E + RT(Z-1) \tag{10}$$

$$\Delta S^R = -R\,ln\frac{V}{V-b} + R\,ln Z + \frac{\partial a}{\partial T}E \tag{11}$$

$$\Delta F^R = RT\,ln\frac{V}{V-b} - RT\,ln Z - aE \tag{12}$$

$$\Delta G^R = RT\,ln\frac{V}{V-b} + RT(Z-1) - RT\,ln Z - aE \tag{13}$$

$$ln\,\varphi = ln\frac{V}{V-b} + Z - 1 - ln Z - \frac{a}{RT}E \tag{14}$$

$$W_S = \left[-\frac{C_P}{C_V}\,\frac{V^2}{M}\left(\frac{\partial P}{\partial V}\right)_T\right]^{0,5} \tag{15}$$

$$\Delta C_V^R = \left[\frac{\partial(\Delta U^R)}{\partial T}\right]_V = T\frac{\partial^2 a}{\partial T^2}E \tag{16}$$

$$\Delta C_P^R = \Delta C_V^R - T\frac{(\partial P/\partial T)_V^2}{(\partial P/\partial V)_T} - R \tag{17}$$

with

$$E = \frac{1}{2\sqrt{-c}}\,ln\frac{V-d+\sqrt{-c}}{V-d-\sqrt{-c}}; \qquad \text{for } c<0 \tag{18a}$$

$$E = \frac{1}{\sqrt{c}}\,arctg\frac{\sqrt{c}}{V-d}; \qquad \text{for } c>0 \tag{18b}$$

$$E = \frac{1}{V-d}; \qquad \text{for } c=0 \tag{18c}$$

The above expressions of the residual departure functions based on GEOS equation may be also used for other cubic equations, which can be converted to the GEOS form. The values of the thermodynamic functions are calculated from:

$$Y = Y^* + \Delta Y^R \tag{19}$$

where Y^* is the ideal gas contribution.

Results and discussions

The knowledge of PVT and thermodynamic properties of hydrofluorocarbons (HFCs) is of importance in relation to their use as refrigerants.

Five equations of state have been used in this work, to calculate the phase equilibrium and the thermodynamic properties for **R143a** (CF_3CH_3) and **R152a** (CHF_2CH_3): Soave-Redlich-Kwong (SRK), Peng-Robinson (PR), Schmidt-Wenzel (SW), Freze et al. (C1) and GEOS3C. The investigated PVT range covers single-phase (liquid or gas) and two-phase (liquid-vapour) regions, using recommended NIST data. The calculations were made

Table 1
VALUES OF C_1, C_2 AND C_3 PARAMETERS FOR **R143a** (CF_3CH_3) AND **R152a** (CHF_2CH_3). CRITICAL DATA AND ACENTRIC FACTORS FROM NIST DATABASE [14]

Component	C_1	C_2	C_3	T range (K)	P range (bar)
R143a (CF_3CH_3)	0.2464	0.8819	-0.8637	161.34–345.86	0.01 – 37.6
R152a(CHF_2CH_3)	0.2733	0.7819	-0.6391	154.56 – 386.41	6.4e-4 – 45.168

Table 2
PVT AND THERMODYNAMIC FUNCTION DEVIATIONS ON THE SATURATION CURVE FOR **R143**a. TEMPERATURE RANGE (K): 161.34–345.86. PRESSURE RANGE (BAR): 0.01 – 37.6 . NUMBER OF DATA POINTS: 94

	AAD (%)				AAD			
EOS	P^S	V^L	V^V	$\Delta_{vap}H$	H^L (kJ/kg)	H^V (kJ/kg)	S^L (kJ/kg/K)	S^V (kJ/kg/K)
SRK	2.30	22.0	4.05	3.30	4.54	5.98	0.01	0.02
PR	0.53	8.14	2.00	2.31	3.28	4.62	0.01	0.02
SW	1.00	10.7	3.09	2.53	2.45	5.32	0.01	0.02
C1	2.00	5.37	3.61	2.82	3.32	6.20	0.01	0.02
GEOS3C	0.31	3.70	2.08	2.61	5.70	2.73	0.02	0.01

with the software package PHEQ (Phase Equilibria) developed in our laboratory [17].

The values of the parameters C_1, C_2 and C_3 of the GEOS3C equation for the two refrigerants are presented in table 1.

The following thermodynamic properties have been predicted: compressibility factor, *Z*; enthalpy, *H*; enthalpy of vaporisation, $\Delta^v H$; entropy, *S*; heat capacity at constant pressure, C_p; heat capacity at constant volume, C_V; heat capacity ratio, C_p/C_V; speed of sound, *Ws*; fugacity coefficient, φ; Joule-Thomson coefficient, *JT*. No data on these thermodynamic properties were regressed in this work. The ideal gas contribution to the thermodynamic properties was calculated using the heat capacity functions recommended in [18].

The results of the calculations for PVT and thermodynamic properties are summarized in tables 2-7, for the two refrigerants. The average absolute deviations (AAD), between calculated values by EOSs and NIST recommended data are given. For each table the number of data points, the pressure and temperature ranges are indicated. The two-phase region properties have been calculated at temperatures from the triple point to the critical point.

The average absolute deviations for a property *Y* are relative (%):

$$\text{AAD }\% = \frac{\sum_{i=1}^{N} \left|(Y_i^{eos} - Y_i^{\exp}) / Y_i^{\exp}\right| \cdot 100}{N} \qquad (20)$$

excepting the enthalpy and entropy where:

$$\text{AAD } H \text{ (or } S) = \frac{\sum_{i=1}^{N} \left|H_i^{eos} - H_i^{\exp}\right|}{N} \qquad (21)$$

Table 3

THERMODYNAMIC FUNCTION DEVIATIONS AT SATURATION FOR **R143**a. TEMPERATURE RANGE (K): 161.34– 345.86. PRESSURE RANGE (BAR): 0.01 – 37.6 . NUMBER OF DATA POINTS: 94

	AAD (%)							
EOS	C_P^L	C_P^V	$(C_P/C_V)^L$	$(C_P/C_V)^V$	Ws^L	Ws^V	JT^{L*}	JT^V
SRK	10.3	11.9	12.9	2.94	11.4	2.04	62.2	37.6
PR	9.90	12.3	12.6	3.26	10.3	1.04	55.4	37.3
SW	10.2	12.2	12.8	3.19	10.4	1.39	56.3	37.3
C1	9.96	12.3	12.7	3.28	16.3	0.83	65.1	36.9
GEOS3C	10.0	13.2	9.23	5.12	44.8	2.57	47.9	37.3

* AAD% calculated from 90 data points

Table 4

THERMODYNAMIC FUNCTION DEVIATIONS IN SINGLE-PHASE REGION FOR **R143**a. TEMPERATURE RANGE (K): 200 – 650. PRESSURE RANGE (BAR): 0.01–1000. NUMBER OF DATA POINTS: 229

	AAD		AAD (%)				
EOS	*H* kJ/kg/K	*S* kJ/kg	Z	C_P	W_S	C_P/C_V	*JT*
SRK	0.01	5.17	9.39	2.57	4.41	3.86	68.4
PR	0.01	2.40	2.78	2.87	4.15	3.64	55.0
SW	0.02	6.30	4.17	6.07	4.28	4.41	190
C1	0.01	3.08	2.87	2.83	7.11	3.65	88.0
GEOS3C	0.02	5.55	2.95	4.15	20.0	4.07	45.9

Table 5

PVT AND THERMODYNAMIC FUNCTION DEVIATIONS ON THE SATURATION CURVE FOR **R152**a. TEMPERATURE RANGE (K): 154.56 – 386.41. PRESSURE RANGE (BAR): 6.4e-4 – 45.168 . NUMBER OF DATA POINTS: 118

	AAD (%)				AAD			
EOS	P^S	V^L	V^V	$\Delta_{vap}H$	H^L (kJ/kg)	H^V (kJ/kg)	S^L (kJ/kg/K)	S^V (kJ/kg /K)
SRK	3.34	23.9	5.17	3.39	6.65	11.9	0.02	0.04
PR	0.81	9.90	2.21	2.48	6.39	8.00	0.02	0.03
SW	2.31	11.9	4.39	2.51	4.11	8.16	0.02	0.03
C1	2.50	4.92	4.01	2.88	6.37	10.7	0.02	0.04
GEOS3C	0.31	4.28	1.72	2.45	7.71	4.82	0.03	0.02

Table 6

THERMODYNAMIC FUNCTION DEVIATIONS AT SATURATION FOR **R152**a. TEMPERATURE RANGE (K): 154.56 – 386.0. PRESSURE RANGE (MPa): (bar): 6.4e-4 – 45.0.NUMBER OF DATA POINTS: 117

	AAD (%)							
EOS	C_P^L	C_P^V	$(C_P/C_V)^L$	$(C_P/C_V)^V$	Ws^L	Ws^V	JT^{L*}	JT^V
SRK	10.9	9.76	12.6	2.68	8.26	1.98	51.6	38.71
PR	10.8	10.2	12.3	2.90	8.43	1.06	45.0	38.5
SW	10.9	10.1	12.5	2.88	8.53	1.34	48.3	38.4
C1	10.8	10.2	12.4	2.92	12.3	0.85	52.1	38.1
GEOS3C	10.0	11.2	8.96	4.70	54.6	2.41	36.4	38.4

* AAD% calculated from 112 data points

Table 7

THERMODYNAMIC FUNCTION DEVIATIONS IN SINGLE-PHASE REGION FOR **R152**a. TEMPERATURE RANGE (K): 200 – 500. PRESSURE RANGE (bar): 0.01–600. NUMBER OF DATA POINTS: 239

	AAD		AAD (%)				
EOS	*S* kJ/kg/K	*H* kJ/kg	Z	C_P	W_S	C_P/C_V	*JT*
SRK	0.02	6.96	10.5	3.30	3.30	3.89	31.4
PR	0.01	4.12	3.88	3.89	3.57	3.72	31.6
SW	0.01	3.86	4.94	4.70	3.61	4.07	40.9
C1	0.02	5.11	2.16	3.97	5.90	3.74	38.6
GEOS3C	0.02	4.90	2.86	4.78	26.1	3.98	30.2

The following observations can be made on the basis of the results of the tables 2-7.

- vapor pressures and saturated volumes are better predicted by GEOS3C, compared to the results obtained using other equations. Surprisingly small are the deviations in vapor pressure predicted by PR equation.

- The liquid volumes calculated with the SRK equation are in poor agreement with experimental data (22% and 24% average deviation). The vapor volume is well reproduced by all five equations of state.

- equations SRK and PR can be used with the same temperature function with three parameters like the GEOS3C equation (eqs. 3-5). This fact leads to better values for vapor pressures but the values of saturated volumes can not be improved without a translation procedure [1]. The advantage of the GEOS3C equation is that the prediction of liquid volume is improved without translation by the parameter C_1 [6].

- GEOS3C equation predicts better results for the enthalpies and the entropies in the vapour phase and also for the heat capacity ratio and Joule-Thomson (JT) coefficient in the liquid phase, on the saturation curve. The AAD% given in tables 3 and 6 for the JT coefficient in the saturated liquid range are relatively high, determined by very small values of the NIST JT coefficients at temperatures where the function changes the sign.

- speeds of sound values predicted by GEOS3C have large errors in comparison with NIST recommended data. As can be seen from the eq. (15), the value of W_s (speed of sound) is depending of both heat capacity ratio and the derivative $\left(\frac{\partial P}{\partial V}\right)_T$. The GEOS3C equation predicts better the heat capacity ratio, but the derivative $\left(\frac{\partial P}{\partial V}\right)_T$ has higher errors. From this analysis results that the correlation of vapor pressures and saturated liquid density does not guarantee accurate values of the derivative $\left(\frac{\partial P}{\partial V}\right)_T$ in the liquid region.

- difference in performance between the EOSs is less noticeable for other thermodynamic properties: enthalpy of vaporization, liquid enthalpy and entropy on the saturation curve and in the single phase region, the both isochoric and isobaric heat capacities in the entire range of T and P, the speed of sound and the Joule-Thomson coefficient for liquid on the saturation curve.

Examples of calculated properties are presented in the figures 1 - 8. Figures 1 and 2 show the pressure – density diagrams for **R143a**. Points figure NIST data, while the curves are calculated with the GEOS3C and SRK equations, for the saturation region and subcritical and supercritical isotherms. Large deviations can be observed in the saturated liquid densities predicted by the SRK equation in comparison with NIST recommended data. The same situation is in the single phase region, on the subcritical isotherms: the densities calculated with the GEOS3C equation are in better agreement with the experimental data in comparison with the densities calculated with the SRK equation.

A comparison of the calculated enthalpies by GEOS3C and C1 equations, on the saturation curve and in the single phase region is shown in figure 3 (points: NIST recommended data). The both equations give good predicted values of enthalpies in the entire range of T and P.

The heat capacity, C_p, prediction from GEOS3C equation, on the saturation curve and in the single phase region is shown in the figure 4. All five equations of state perform similarly for this property and predict correctly an infinite value for isobaric heat capacity at the critical point. As a “memory” effect of this behavior, a maximum in the C_p

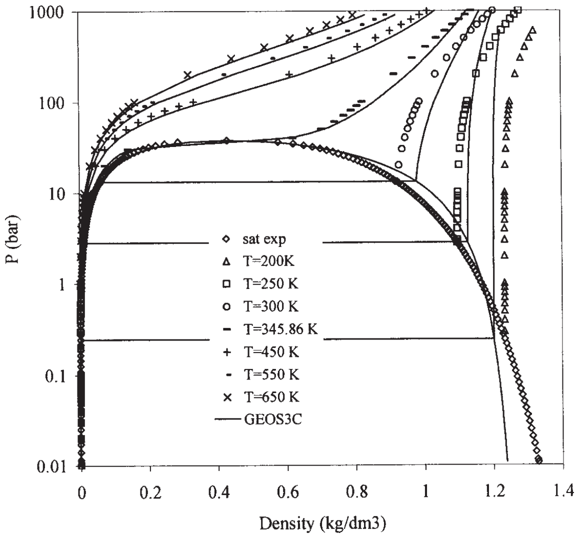

Fig. 1. Pressure-density diagram for **R143a**. Points: NIST data [14]. Prediction with the GEOS3C equation.

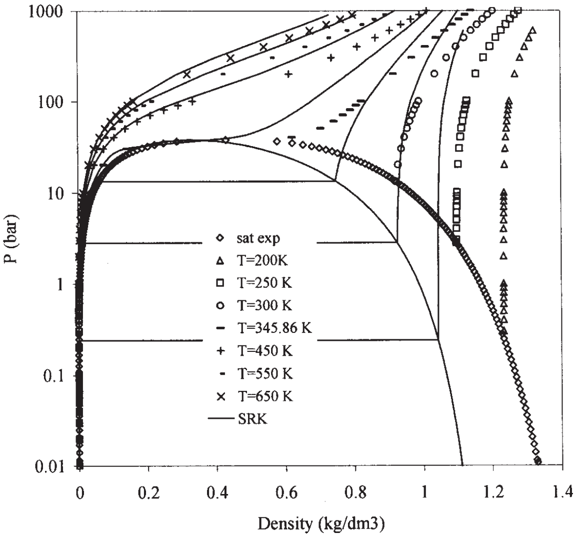

Fig. 2. Pressure-density diagram for **R143a**. Points: NIST data [14]. Prediction with the SRK equation

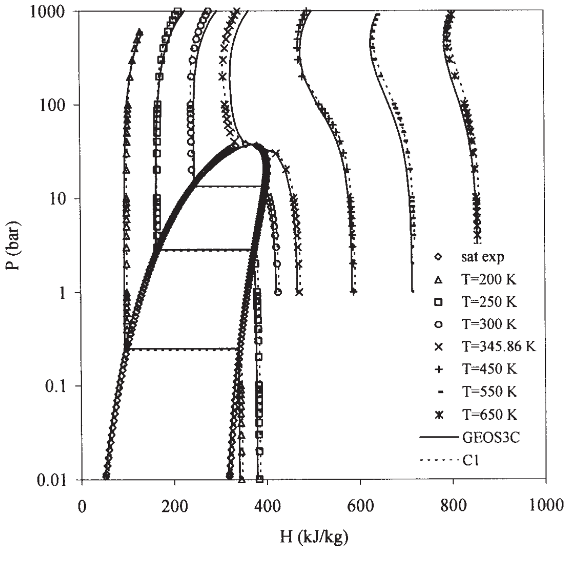

Fig. 3. Pressure-enthalpy diagram for **R143a**. Points: NIST data [14]. Prediction with the GEOS3C and C1 equations

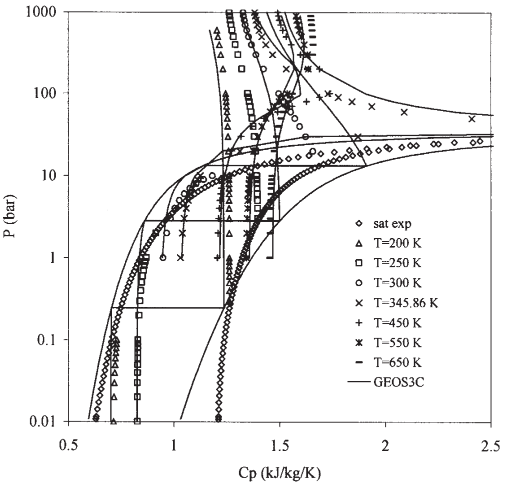

Fig. 4. Pressure-heat capacity diagram for **R143a**. Points: NIST data [14]. Prediction with the GEOS3C equation

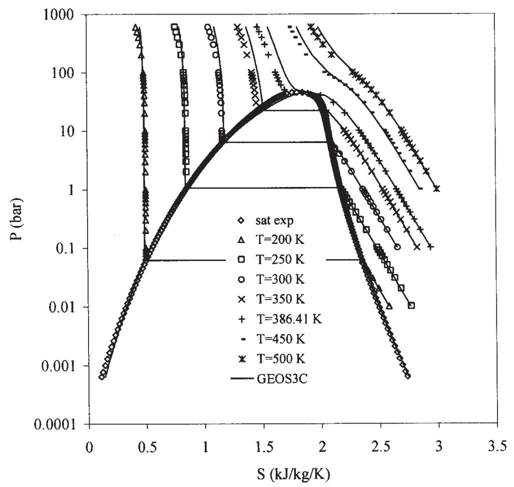

Fig. 5. Pressure-entropy diagram for **R152a**. Points: NIST data [14]. Prediction with the GEOS3C equation

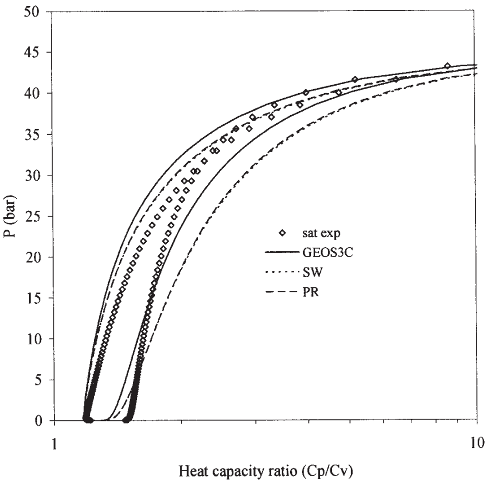

Fig. 6. Pressure-heat capacity ratio saturation curve for **R152a**. Points: NIST data [14]. Prediction with the GEOS3C, SW and PR equations

function is predicted on the supercritical isotherms.

The pressure – entropy diagram of **R152a** calculated by GEOS3C is presented in figure 5. The calculated values are in good agreement with the NIST data. All other equations of state perform similarly.

The heat capacity ratio predictions by GEOS3C, SW and PR equations for **R152a** on the saturation curve are

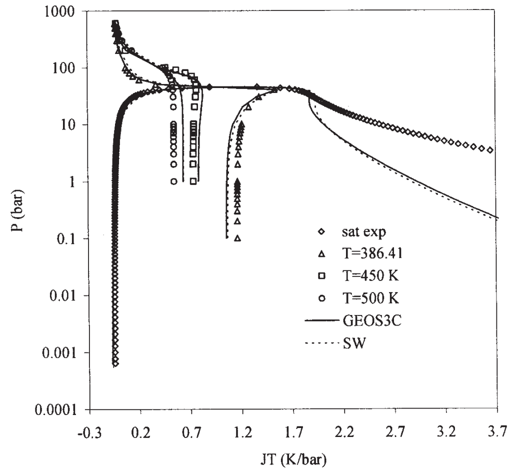

Fig. 7. Joule Thomson coefficient prediction for **R152a** by GEOS3C and SW equations. Points: NIST data [14]

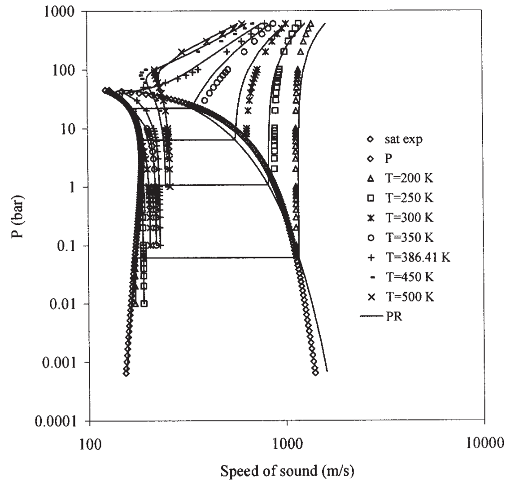

Fig. 8. Pressure-speed of sound diagram for **R152a**. Points: NIST data [14]. Prediction with the PR equation

presented in figure 6. The results obtained by GEOS3C are in a better agreement with the NIST data, in comparison with the SW and PR equations.

The Joule-Thomson coefficient predictions for **R152a** from the GEOS3C and SW equations on the saturation curve and in the single phase region are presented in figure 7. A satisfactory agreement with NIST data may be remarked.

Figure 8 shows the pressure – speed of sound diagram for **R152a**, in the entire range of *T* and *P*. The predicted values are in good agreement with the NIST data for this refrigerant.

On the basis of the studied HFCs (**R143a** and **R152a**), it is possible to conclude that GEOS3C predict better PVT properties and all five EOS's predict consistent results apart from the failure to give an infinite value for the isochoric heat capacity (C_V) at the critical point.

Conclusions

The vapour – liquid equilibrium and the thermodynamic properties of refrigerants **R143a** and **R152a** were predicted by five equations of state SRK, PR, SW, C1 and GEOS3C on a wide PVT range, including the entire saturation region. A large comparison with PVT and equilibrium recommended NIST data was made.

The following thermodynamic properties were calculated: compressibility factor, *Z*; enthalpy, *H*; enthalpy of vaporisation, $\Delta^v H$; entropy, *S*; heat capacity at constant pressure, C_P; heat capacity at constant volume, C_V; heat capacity ratio, C_P/C_V; speed of sound, *Ws*; fugacity coefficient, φ; Joule-Thomson coefficient, *JT*. The comparisons with recommended literature data for these properties were also presented.

The GEOS3C equation gives better predictions of vapor pressure and saturated liquid volume than the other equations of state. The saturated vapour volume is well reproduced by all five equations of state.

Regarding the thermodynamic properties, the GEOS3C equation predicts better results for the enthalpies and the entropies in the vapour phase and also for the adiabatic index and Joule Thomson coefficient in the liquid phase, on the saturation curve. The speeds of sound values predicted by GEOS3C have large errors in comparison with NIST recommended data.

The difference in performance between the five EOSs is less noticeable for other thermodynamic properties: enthalpy of vaporization, liquid enthalpy and entropy on the saturation curve and in the single phase region, both isochoric and isobaric heat capacities in the entire range of *T* and *P*, the speed of sound and the Joule Thompson coefficient for liquid on the saturation curve.

So far GEOS3C, with three estimated parameters, compares favorably to other equations in literature, being simple enough for applications.

Acknowledgements: The authors are grateful to National Council for Scientific Research of Romania, for financial support.

List of symbols

a, b, c, d - parameters in GEOS
AAD - absolute average deviation
B - dimensionless parameter in GEOS, defined by eq. (7)
C_1, C_2 and C_3 - parameters in GEOS3C temperature function
C_V, C_P - isochoric and isobaric heat capacities
E - expression based on GEOS, defined by eq. (18)
F - Helmholtz function
H - enthalpy
JT - Joule-Thomson coefficient
M - molar mass
P, P^S - pressure, saturation pressure
R - universal gaz constant
S - entropy
T - temperature
U - internal energy
V, V^L, V^V - molar volume, liquid volume, vapor volume
*W*s - speed of sound
Y - thermodynamic function (general notation)
Z - compresibility factor

Greeks

α_c - Riedel's criterium (parameter in GEOS)
β- reduced temperature function in GEOS
φ - fugacity coefficient
Ω_a, Ω_b, Ω_c, Ω_d - parameters of GEOS
ω - acentric factor

Subscripts

c - critical property
r - reduced property

Superscript

exp - experimental (NIST recommended) data
eos - calculated values

References

1. GEANĂ D., FEROIU V., Equations of State. Applications to Phase Equilibria, Ed. Tehnică (ISBN 973-31-1447-2), Bucureşti, 2000
2. ESLAMI H., N. MEHDIPOURB N., BOUSHEHRIB A., International Journal of Refrigeration, 29 (1), 2006, p. 150
3. MADANIA H., VALTZ A., COQUELET C., MENIAIA A. H., RICHON D., Fluid Phase Equilibria, 268, 2008, p. 68
4. CHEN Q., HONG R., CHEN G., Fluid Phase Equilibria, 269, 2008, p. 113
5. JU M., YUN Y., SHIN M. S., KIM H., J. Chem. Thermodynamics, 41, 2009, p. 1339
6. GEANĂ D., V. FEROIU V., Fluid Phase Equilibria, 174, 2000, p. 51.
7. FEROIU V., GEANĂ D., Fluid Phase Equilibria, 207, 2003, p. 283
8. FEROIU V., GEANĂ D., SECUIANU C., Rev. Chim. (Bucharest), **59,** no.5, 2008, p. 554
9. SOAVE G., Chem. Eng. Sci., 27, 1972, p. 1197
10. PENG D. Y., ROBINSON D. B., Ind. Eng. Chem. Fundam., 15, 1976, p. 59
11. SCHMIDT G., WENZEL H., Chem. Eng. Sci., 35, 1980, p. 1503
12. FREZE R., CHEVALIER J. L., PENELOUX A., RAUZY E., Fluid Phase Equilibria, 15, 1983, p. 33.
13. GEANĂ D., FEROIU V., Proceedings of the National Conference on Chemistry and Chemical Engineering, Bucharest, Romania, oct. 1995, vol. 3, p. 133
14. NIST - Thermophysical Properties of Fluid Systems, Database 2010, http://webbook.nist.gov/chemistry/fluid/.
15. GEANĂ D., Rev. Chim. (Bucharest), **37**, no. 5, 1986, p. 303; **37,** no. 11, 1986, p. 951; **38**, 1987, p. 975
16. D. GEANĂ, R. TĂNĂSESCU, Rev. Chim. (Bucharest), **40**, 1989, p. 682
17. GEANĂ D., RUS L., Proceeding of the Romanian International Conference on Chemistry and Chemical Engineering (RICCCE XIV), Bucharest, Romania, oct. 2005, vol. 2 p. 170; www.chfiz.pub.ro/laboratories/trl/myweb/termod
18. REID, R., PRAUSNITZ, J.M., POLING, B., The Properties of Gases and Liquids, McGraw-Hill, New York, 1986

Manuscript received: 15.03.2011